

---

Faculty of Engineering

Faculty Publications

---

This is a post-print version of the following article:

Current State of Modern Rammed Construction: A Case Study of First Peoples House After 7 Years Exposure

Allan Kailey & Rishi Gupta

October 2015

The final publication is available via Scientific.Net at:

<https://doi.org/10.4028/www.scientific.net/KEM.666.63>

---

Citation for this paper:

Kailey, A., & Gupta R. (2015). Current State of Modern Rammed Construction: A Case Study of First Peoples House After 7 Years Exposure. *Key Engineering Materials*, 666, 63-76.  
<https://doi.org/10.4028/www.scientific.net/KEM.666.63>.

# Current State of Modern Rammed Construction: A Case Study of First Peoples House After 7 Years Exposure

Allan Kailey<sup>1, a</sup> and Gupta Rishi<sup>1, b</sup>

<sup>1</sup>Department of Mechanical Engineering, University of Victoria, 3800 Finnerty Road, Victoria, BC, Canada

<sup>a</sup>kaileya@uvic.ca, <sup>b</sup>guptar@uvic.ca

**Keywords:** Rammed earth, sustainability, rebound hammer, thermal imaging, deterioration

**Abstract.** This paper presents a study on the current condition of the First Peoples House, located at the University of Victoria in British Columbia. The building houses two rammed earth walls that exemplify the use of stabilized rammed earth as a modern construction material. These rammed earth walls have been exposed to 7 years of natural weathering in a wet climate. A rebound hammer, infrared camera, and a new method developed to quantify surface deterioration were used in Non-Destructive Testing (NDT). The results provided insight into the compressive strength, thermal envelope and surface condition of the walls. Relationships between wind direction and wind speed are presented. It is postulated that the wall that is most exposed to a combination of both effects will exhibit the largest forms of deterioration. This hypothesis was addressed using results from NDT and local wind data.

## Introduction

Reinforced or Stabilized Rammed Earth (SRE) is a relatively modern construction technique that has evolved from an ancient and proven technology, where locally available soil is compacted between formwork to create an earthen wall. This technique dates as far back to the construction of the Great Wall of China [1]; many structures still stand today. Interest in RE was eventually suppressed by the use of concrete and steel for their strength properties however, RE is currently being revived. The SIREWALL system is one example of this development, where RE is strengthened with rebar and additives such as, cement or lime. Rigid insulation is often found down the wall center for improved living comfort and thermal efficiency [2]. SRE is gaining widespread popularity for its sustainability and lower environmental impact when compared to other building materials. A 10% cement SRE wall has 75% lower production energy than a steel-framed wall [3]. Using local soils also eliminates the need to transport material over long distances, which supports reducing CO<sub>2</sub> emissions. However, the sustainability of RE is slightly decreased with the use of cement, since the cement industry contributes 5-7% of global CO<sub>2</sub> emissions [4]. Regardless, the benefits of SRE are outweighing some of the other building materials in our society that is becoming more dedicated to sustainable living.

British Columbia (BC) is becoming a hot-spot for SRE construction; the NK'Mip Desert Cultural Centre stands beautifully in Osoyoos as the largest insulated RE wall in the world (80m x 0.6m x 5.5m), and at least 30 custom designed residential homes are located on Salt Spring Island [7]. SIREWALL has an impressive construction portfolio including work completed for The Edmonton Valley Zoo in Alberta and Grand Beach Washrooms in Manitoba. The number of SRE buildings is increasing worldwide such as, in China (Naked Staples Project), India (Mangar Hotel Project) and the United States (Sublette County Library Project) [2]. SRE is primarily used in residential construction however, SIREWALL's project portfolio consists of many commercial applications that support the evolution of RE into a competitive building material.

## Project Motivation

The current state of modern RE structures in BC is unknown. It is unclear whether SRE will experience the same longevity as the ancient structures remaining today. It is a question of whether the SRE walls at the University of Victoria's (UVic) First Peoples House (FPH) have felt the effects of environmental weathering such as, wind loading and precipitation over the period of its 7 year life. Facilities Management at UVic is responsible for maintaining the state of the walls. Currently, no known documentation exists for a future maintenance plan. This article acts as the first piece of technical information to discuss the current state of the SRE walls and to promote a future maintenance strategy for UVic and for other similar structures around the world. Additionally, the insulating ability of the FPH is to be further explored, as SRE is continuously being considered for use in thermally efficient buildings [3]. It is therefore of interest to advance the research on SRE construction by analyzing the FPH, and to provide literature that will aid in the development of future SRE technology.

## First Peoples House

The First Peoples House (FPH) was constructed in 2008. It provides a welcoming community space, and an academic and cultural centre for Indigenous students [6]. It is one of the many LEED Gold certified buildings on campus; showcasing UVic's commitment to design and sustainability through the use of recycled material such as, reclaimed red cedar, steel reinforcement and SRE (Figure 1). A number of other features include a green roof, natural light in 90% of the building, landscaping, and a storm retention pond fed by roof run off.



**Figure 1. First Peoples House, view of rear entrance**

The FPH consists of two SRE walls that are situated on the eastern most and western most faces of the building corresponding to the main and rear pedestrian entrances (Figure 2). Both walls are 500mm thick, and exterior-interior sections have a 100mm thick central cavity for insulation. Internal steel reinforcement is used for added strength. The outside visible surface area of Wall #1, the eastern most wall, is approximately 9.98m x 3.53m. It is shielded by shrubbery and an adjacent wall that extends from the main entrance. Half of this wall is an exterior-exterior wall and the other half is an exterior-interior wall. The western most wall, Wall #2, has an outside visible surface area of 10.00m x 3.39m. It is a fully exterior-interior wall with little protection from the environment.

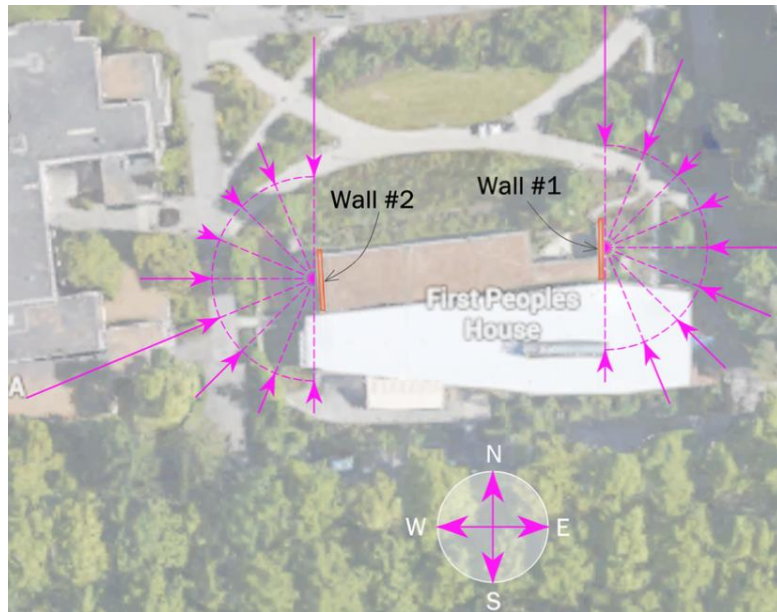


**Figure 2. Location of rammed earth walls with historical wind data**

## Literature Review

A number of condition assessments have been performed on older RE construction however, none seem to address RE constructed within the last 10 years. It is likely that condition assessments are not yet deemed necessary, as newer RE has yet to display significant forms of aging to justify an assessment.

Liang analyzed five Hakka RE buildings in the Fujian Province of China using non-destructive testing [7]. The buildings were constructed between 1662-1706, and are an incredible example of the longevity of ancient RE. Compressive strength was quantified using an ultrasonic device and rebound hammer. It was found that the ultrasonic device more accurately represented the true strength properties. The highest compressive strength was observed in the material that contained the largest amount of lime. Since lime is used as a strengthening agent in RE, these results agree. An infrared camera was used to quantify the thermal building envelope, but was unsuccessful due to poor equipment sensitivity. The results obtained are only conclusive of ancient RE technology however, the NDT performed can be used to assess the integrity of newer SRE.

Another assessment approach was developed by Bui, where a method of stereo-photogrammetry was used to quantify the erosion depth of SRE walls exposed to 20 years of weathering [1]. Two photos were taken from two different viewing angles and superimposed to form a 3D relief that displayed measurable erosion depth. The measurements from the photos were accurate within  $\pm 0.005\text{mm}$ . As predicted, RE that had been stabilized with natural hydraulic lime showed minimal erosion compared to unstabilized RE.

The properties of RE are heavily dependent on its composition such as, soil and moisture content, percent lime and cement content etc. This composition is often selected based on the environment it will be operating in. A dry climate will have different requirements than a wet climate. Results obtained from other NDT tests found in literature cannot be used to determine the state of the FPH because RE is unique and specific to its operating environment and material composition.

## Non-Destructive Evaluation

The current condition of the FPH can be investigated using NDT to evaluate the material and structural properties without harming the building. In this study, a rebound hammer, infrared camera and high resolution camera were employed to assess the surface strength, thermal building envelope, and surface deterioration of RE. Methods using the rebound hammer and infrared camera were previously developed by Liang [7], and the high resolution camera method has yet to be documented in literature. Table 1 summarizes the specific test equipment used.

**Table 1. Test equipment used**

Device	Accuracy
Proceq Concrete Test Hammer (Original Schmidt) Model N	$\pm 4.5\text{-}8 \text{ Nmm}^2$
Flir I7 Infrared Camera	$\pm 2\%$
Canon 5D Mark 11 high resolution camera	21 megapixels

Points were marked on the outside surface of each wall, according to Figure 3, where measurements would be taken. The same points were marked on the inside surface using physical measurements from a datum. Steel reinforcement is greatest near the foundation and roofline. Locating the points half way up each wall targets the minimum strength, and equally distributing them along the length of the wall captures it's entirety. The one less point on Wall #2 was due to having to work around doors and windows.

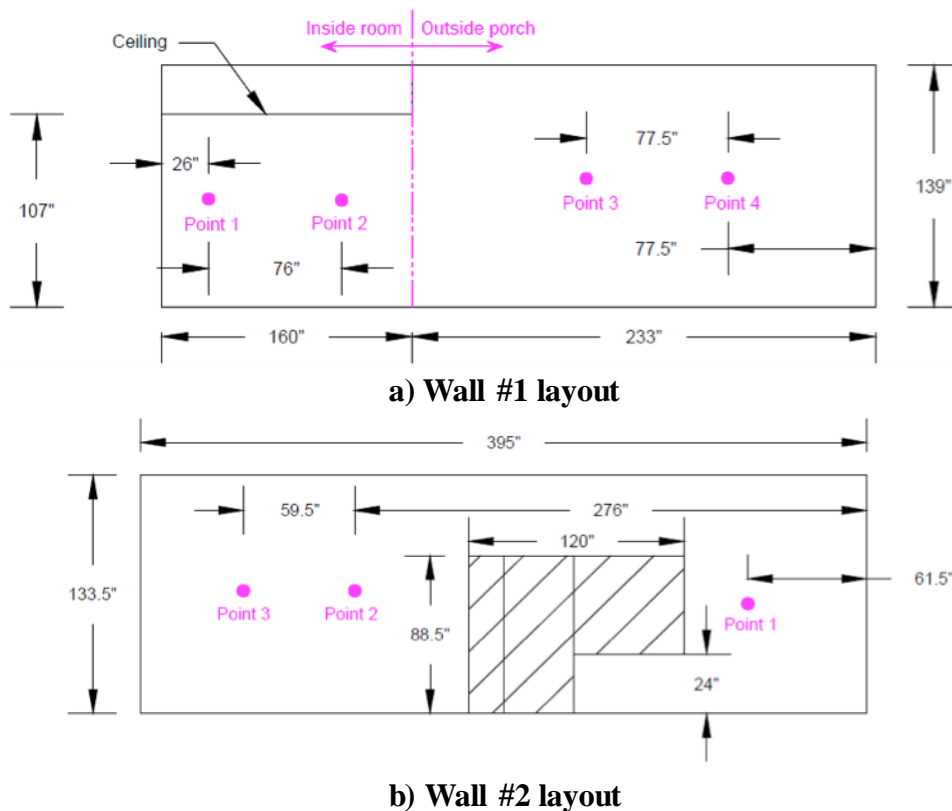


**Figure 3. Wall layouts, view looking at outside surface**

**Principal of Rebound Hammer Method.** A rebound hammer, or Schmidt Hammer, is used to measure the surface strength properties of a concrete or rock wall. The rebound hammer is accepted for use on SRE because of its similarities to concrete. The Model N, designed by Proceq, applies an impact energy of 2.207 Nm. Rebound values are read directly from the built-in scale, and are converted to compressive strengths using the chart provided by the manufacturer [8].

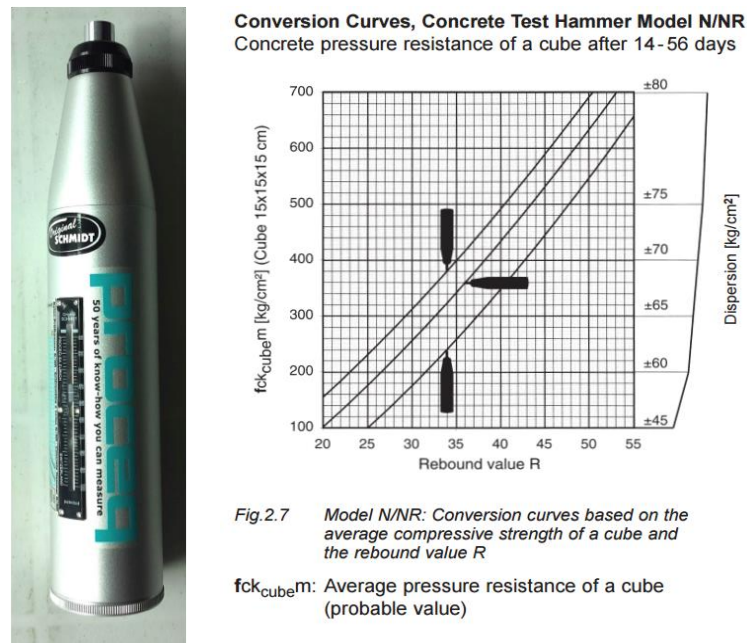


**Figure 4. Rebound hammer (left) and corresponding conversion curve used [8]**

**Compressive Strength Results.** Rainfall had not occurred within the last 24 hours when measurements were taken. Four data points were recorded at each point, and the mean rebound value was used to read the compressive strength conversion chart; this is summarized in

Table 2 and

Table 3.

**Table 2. Wall #1 compressive strength summary**

Point	1	2	3	4
<b>Outside Surface</b>				
Mean rebound value	41.75	37.75	36.67	38.67
Strength [MPa]	51.98	38.25	36.28	40.21
<b>Inside surface</b>				
Mean rebound value	45.13	39.06	36.50	39.33

<b>Strength [MPa]</b>	51.98	38.25	36.28	40.21
<b>Difference [MPa]</b>	6.86	1.96	-0.98	0.00

**Table 3. Wall #2 compressive strength summary**

<b>Point</b>	<b>1</b>	<b>2</b>	<b>3</b>
	<b>Outside Surface</b>		
<b>Mean rebound value</b>	37.50	35.00	30.25
<b>Strength [MPa]</b>	38.25	33.34	25.50
	<b>Inside Surface</b>		
<b>Mean rebound value</b>	40.25	34.63	37.13
<b>Strength [MPa]</b>	43.15	32.36	37.27
<b>Difference [MPa]</b>	4.90	-0.98	11.11

The compressive strengths are again shown in Fig. 5 and Figure for easy visualization. A large difference of 6.86 MPa exists between the outside and inside surfaces at Point 1 on Wall #1. For Wall #2, the largest difference is 11.77 MPa at Point 3.

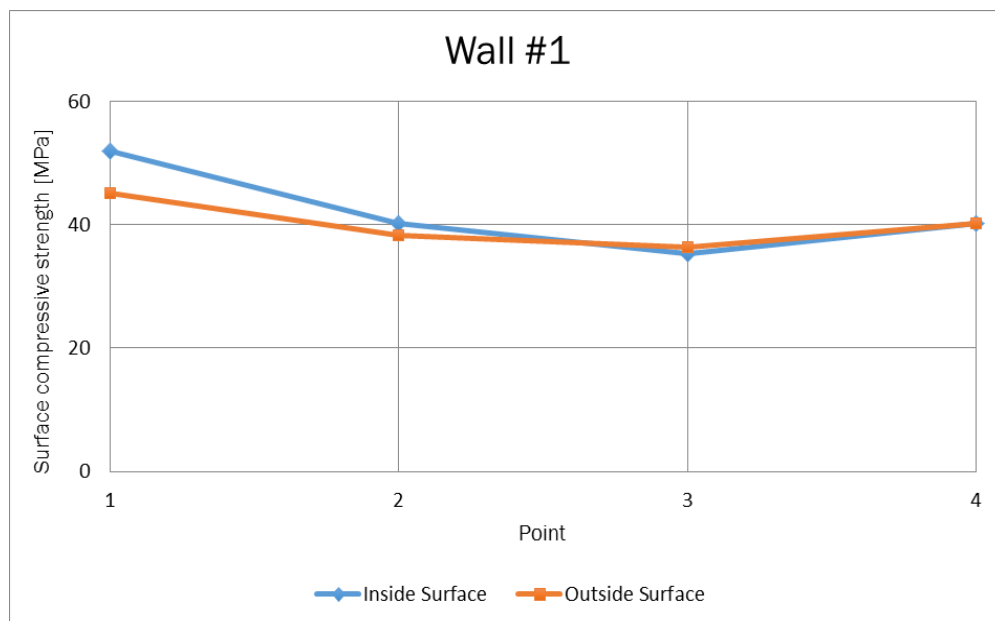


**Figure 5. Compressive strength variation of Wall #1**



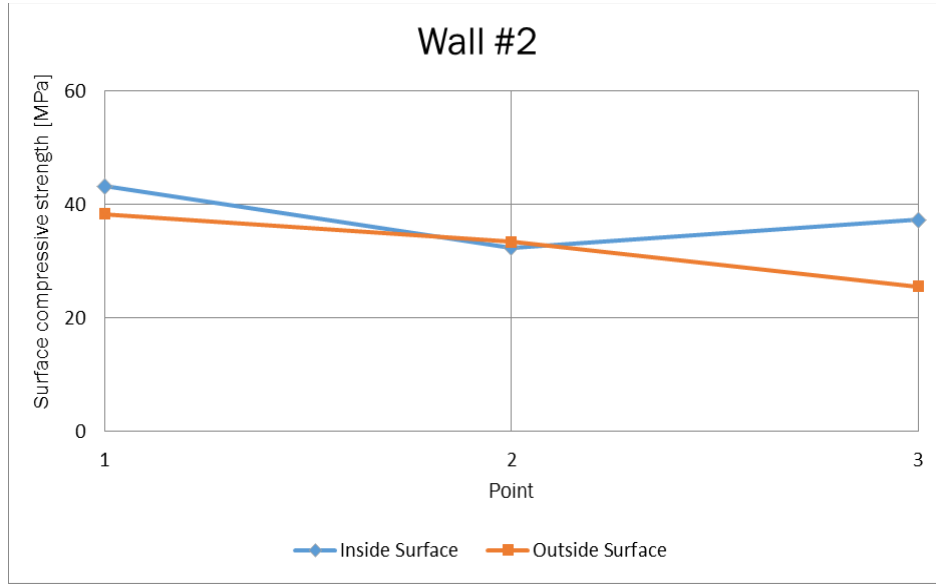


**Figure 6. Compressive strength variation of Wall #2**

The trend seen on Wall #1 shows that the surfaces on exterior-exterior walls (Points 3 and 4) potentially deteriorate at the same rate. This is not surprising, as both surfaces are exposed to the same climate year round. Larger differences are seen on exterior-interior walls (Points 1 and 2). Interior walls are often kept in an environment that is maintained at 20-25°C whereas exterior walls are exposed to fluctuations in temperature and weather. The result is a wall that stays relatively preserved on one side, and is allowed to age on the other.

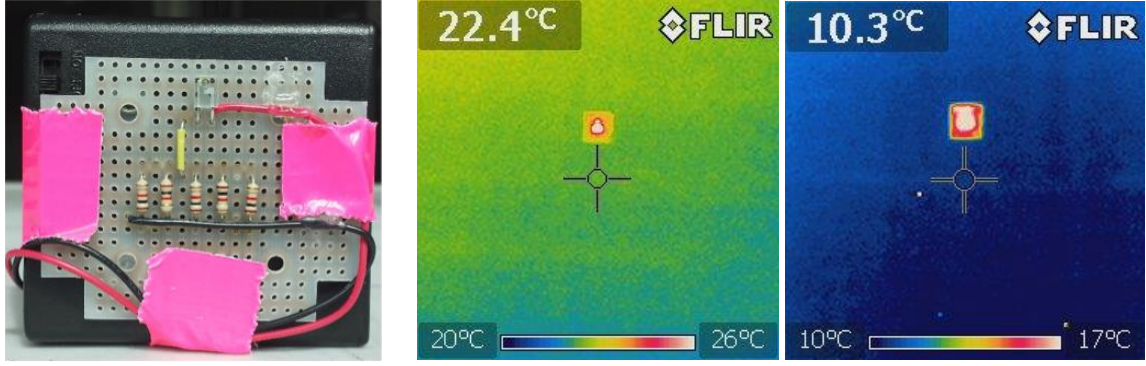
**Principal of Thermal Imaging Method.** An infrared camera can be used to investigate the insulating properties of SRE. The infrared camera operates on the following heat transfer principal (Bergman, Lavine, Incropera, & Dewitt, 2011):

$$q_{rad} = \epsilon \sigma (T_h^4 - T_c^4) A \quad (1)$$

Where the net radiation heat loss,  $q_{rad}$ , is proportional to the temperature of the surface emitting radiation. The infrared camera quantifies radiation heat loss by measuring the wavelength of infrared light reflected from the wall surface. No literature was found on the emissivity,  $\epsilon$ , of SRE. It was assumed to have a similar emissivity to concrete, which is approximately 0.94 [9]. The nearest emissivity that could be specified in the infrared camera was 0.95. The Stefan-Boltzmann constant,  $\sigma$ , is a known physical quantity, and the camera calculates the surface area being viewed,  $A$ , and surrounding environmental temperature,  $T_c$ . The unknown quantity,  $T_h$  is determined as the temperature of the desired surface.

Duct tape has a similar emissivity to SRE and so, it was impossible to locate the marked points on the camera display. A battery powered infrared emitter (frontal dimensions 6.35cm x 6.67cm) was built exclusively for this project to overcome the issue (Figure a). The circuit itself emitted a significant amount of heat and so, it was placed approximately 6 inches above each point as to not skew the readings. The infrared emitter could be clearly identified in the display (Figure b).





a) Infrared circuit built for this study

b) Infrared image of Wall #1, Point 1 inside (left) and outside (right)

**Figure 7. Infrared emitter used**

The temperature readings obtained from the infrared camera were used to determine the heat transfer rate between the inner and outer surfaces [10]. Heat transfer by conduction between two points,  $q_{cond}$ , is related to temperature difference by:

$$q_{cond} = U\Delta T \quad (2)$$

The thermal resistivity,  $U$ , is a property of the RE material and insulation. The  $U$ -value of RE is approximately  $0.339 \text{ W/m}^2\text{K}$  as determined by Hall [11]. This  $U$ -value is based on a 400mm thick SRE wall, with 50mm thick polyurethane board of insulation inserted into the center. It should be noted that the FPH uses 100mm thick insulation; it should exhibit a larger thermal resistance (smaller  $U$ -value) than that discovered by Hall, assuming that the same type of insulation is used. The  $U$ -value is constant everywhere if the material between the outside and inside surfaces is considered constant. By knowing the temperature difference between surfaces and the total resistivity, the heat loss to the surroundings was determined to provide insight into the insulating capability of SRE.

**Surface Temperature Results.** In order to illustrate the effectiveness of SRE as an insulating material, temperature readings were recorded and the conductive heat transfer rate was determined. Temperature was measured at each point on the inside and outside surfaces. A sample thermal image is shown in Figure . The recorded temperatures at each point are visually summarized in Figure and Figure. Point 2 on Wall #1 and Point 3 on Wall #2 exhibited the largest temperature differences, and will therefore experience the largest heat loss.

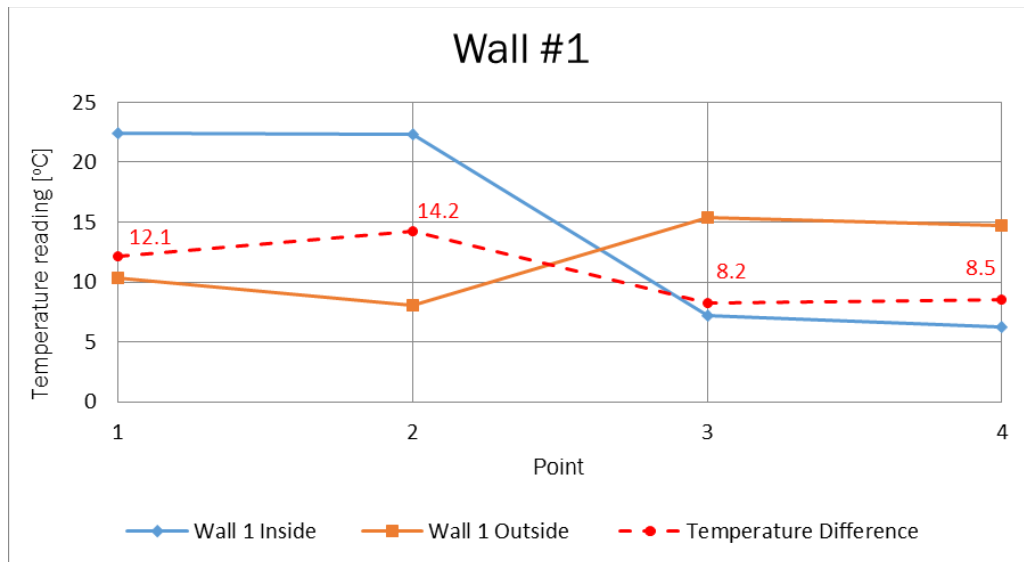


**Figure 8. Surface temperature results for Wall #1**

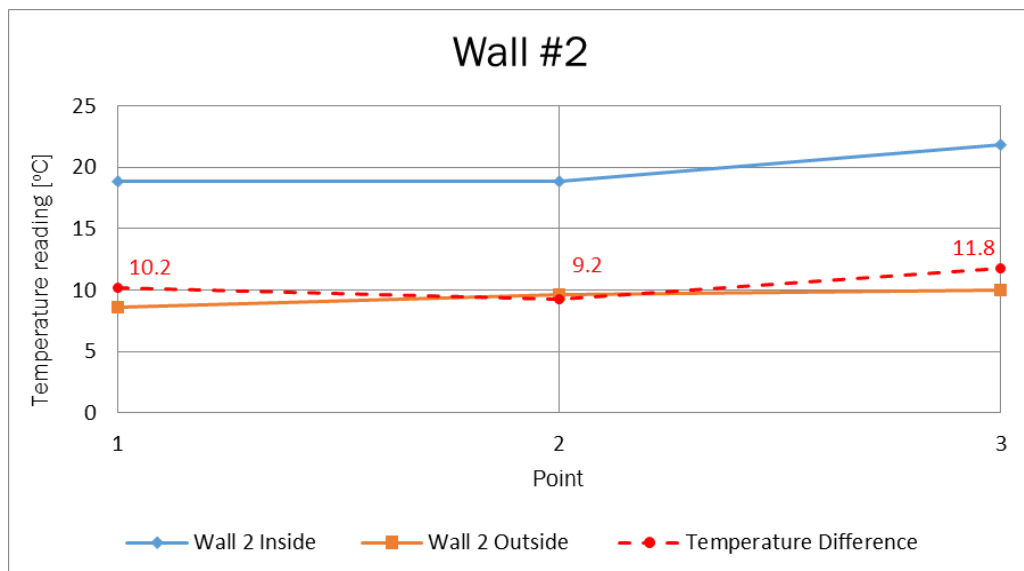


**Figure 9. Surface temperature results for Wall #2**

**Heat Transfer-Density Relationship.** The temperature differences and heat transfer rates are summarized in Table 4. Points 3 and 4 on Wall #1 were excluded because both inside and outside surfaces are exposed to the same environment. Heat transfer rate is related to the density of the medium, where the driving potential is temperature difference. Therefore, heat transfer rate may indicate variations in density. As seen in

**Table 4,** Point 2 on Wall #1 and Point 3 on Wall #2 exhibit the largest heat transfer rates. The material at these locations may be denser, or the insulation less effective than at other locations.

**Table 4. Calculated heat loss/exposed surface area**

	Point	U-value [W/m <sup>2</sup> K]	Difference [°C]	Heat loss [W/m <sup>2</sup> K]	Average heat loss/room [W/ <sup>2</sup> K]
<b>Wall #1</b>	1	0.339	12.1	4.17	4.49
	2	0.339	14.2	4.81	
<b>Wall #2</b>	1	0.339	14.2	4.81	3.42
	2	0.339	9.2	3.08	3.53
	3	0.339	11.8	3.97	

Hall concluded that there exists a relationship between thermal resistance and the moisture content of SRE, where increasing moisture content has a negative impact on the thermal resistance [11]. It is possible that the larger heat transfer rates exist at locations where the moisture content is larger. It should be noted that adjusting moisture content comes at the expense of structural strength. A dry material will be more brittle, which is especially undesirable in the event of an earthquake.

**Principal of High Resolution Photography Method.** Surface deterioration due to weathering can be quantified by photographing an image of known area with a high resolution camera, and then analyzing the image to determine the total area of deterioration. By adjusting the color, contrast, shadow and other image properties, the cracks, porosity and pitting can be clearly defined. AutoCAD 2013 was used to draw closed-loop splines around prominently deteriorated regions. A single “hatch” filled the enclosed sketches, and the “area” command was used to determine the total area of the hatched, or deteriorated regions. Surface deterioration can then be quantified as percent of total surface area. Images used in the analysis were Figure .

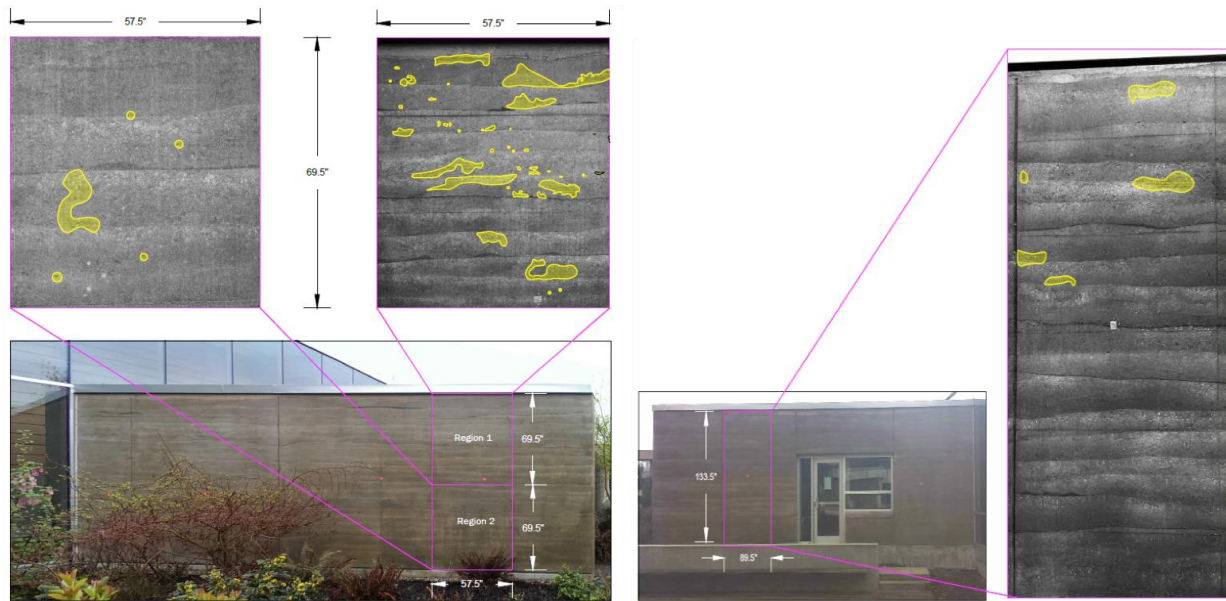


**Figure 10. Wall #1 (left) and Wall #2 (right) surface deterioration analysis**

**Surface Deterioration and Visual Inspection Results.** The wall section analyzed best represented the overall condition of the wall. This was determined by visual inspection, with no relationship between the chosen section and the marked points. The walls were photographed from approximately 4m away, and the results are presented in Table 5. Wall #1 shows an overall surface area deterioration of 3.69%, and Wall #2 as 1.78%.

**Table 5. Percent outside surface deteriorated of Wall #1 and Wall #2**

	Size [m]	Total area [m <sup>2</sup> ]	Deteriorated area [m <sup>2</sup> ]	% Deteriorated
<b>Wall #1</b>				
<b>Region 1</b>	1.46 x 1.76	2.58	0.06	2.33
<b>Region 2</b>	1.46 x 1.76	2.58	0.17	6.59
<b>Total</b>	9.98 x 3.53	35.2	1.30	<b>3.96</b>
<b>Wall #2</b>				
<b>Region 1</b>	2.27 x 3.39	7.71	0.14	1.78
<b>Total</b>	10.0 x 2.8	28.13	0.60	<b>1.78</b>

A deterioration analysis was not performed on the inside surfaces because they were well preserved, having never been exposed to the outside environment. However, all interior walls showed significant signs of efflorescence at cracks and other defect sites, as shown in Figure. Efflorescence is a result of moisture migration through a material to bring soluble salts to the surface. The appearance is a white powder, and is often found on poorly sealed concrete. Moisture penetration to RE can occur in a number of ways: wind-driven rainfall, cyclic wetting and drying, poor thermal performance, loss of adhesion between binding aggregates and metal corrosion [12]. Mechanisms that could promote moisture transmission are capillary suction, gravity and hydrostatic pressure. This potentially

explains why efflorescence does not exist on the exterior-exterior wall; no pressure differential would exist to drive the movement of moisture.



**Figure 11. Signs of efflorescence on inside surface of Wall #1**

Six rust sites exist on the outside surface of Wall #2. As seen in Figure , a linear relationship exists between the site locations. It is likely that these sites correlate to the placement of interior rebar. If not, formwork during construction could have left small rust deposits on the surface.



**Figure 12. Rust sites on outside surface of Wall #2**

### **Environmental Effects and NDT Results**

The results from the NDT tests encourage an investigation into environmental effects that might cause certain sections of a wall to deteriorate faster than others, both structurally and aesthetically. Wind direction and magnitude are predicted to have the greatest effect on these parameters. Wall #1 and Wall #2 are located on opposite faces of the building; they are exposed to entirely different wind directions. Wind direction and wind speed data was obtained from the nearest wind station (WMO ID: 71783) located at 48°27'25.200" N latitude, 123°18'16.600" W longitude [13]. This location corresponds to the Bob Wright Building on campus, as shown in Figure. Data was obtained from



2008-2015 and used to plot Figure 2, where the length of the arrows is proportional to the number of hours of wind seen at that direction.



**Figure 13. Orientation of First Peoples House with respect to wind data collection**

Total wind hours and wind speed is plotted per direction in Figure. Wind direction is expressed in degrees, where  $360^\circ$  means a wind blowing from the geographic North Pole. The largest number of hours observed with respect to the greatest wind speed is seen between  $240^\circ$ - $270^\circ$ .

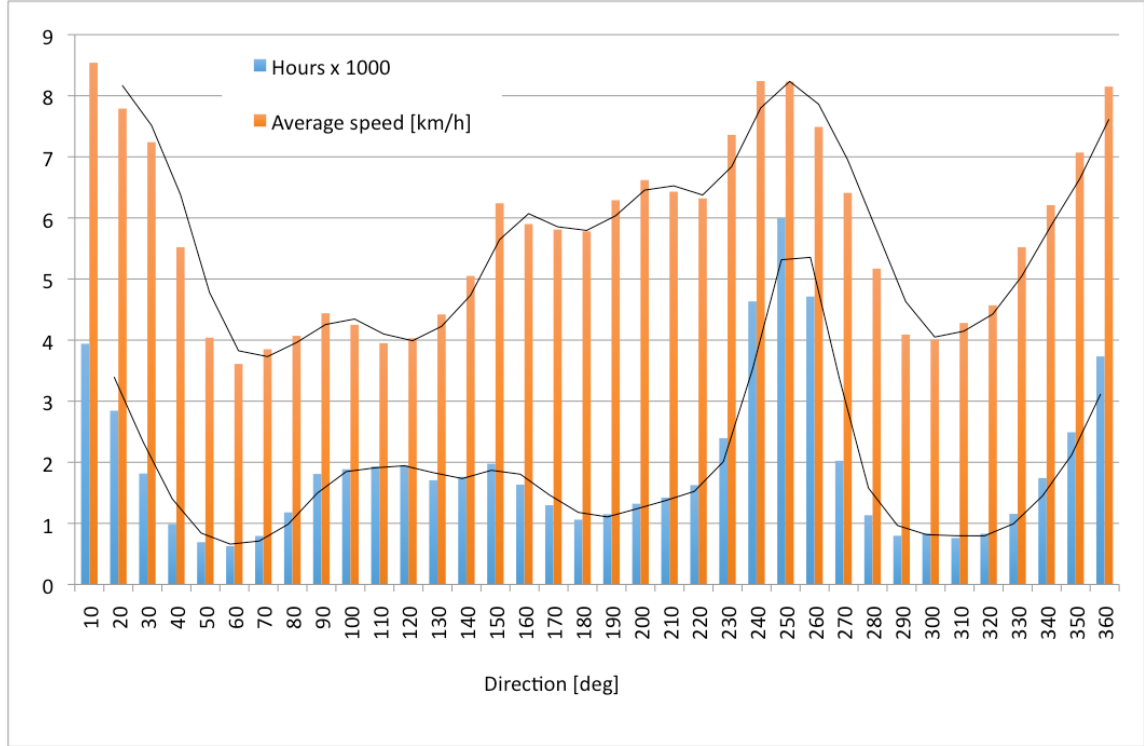


**Figure 14. Number of hours and average wind speed recorded between 2008-2015**

In general terms, the hypothesis that wind speed is proportional to wind loading is based on the law of conservation of linear momentum. A moving fluid (or body) exerts a force on a control surface that is equal to the difference between the entering and leaving momentum of that surface [14]. For a steady system, this is represented in literature as:

$$\sum F_{cv} = \left( \sum \dot{m}V \right)_{in} - \left( \sum \dot{m}V \right)_{out} \quad (3)$$

If the control surface is considered as the outside surface of the wall, than the outlet momentum is negligible compared to the inlet. The force exerted on the wall (control surface) is then proportional to the product of the incoming mass flow and velocity of air. If wind loading is proportional to wind speed, and if wind loading is related to surface and structural deterioration, then wind speed must also have a similar relationship to deterioration. If this hypothesis is correct, then Wall #2 should exhibit less strength and more surface erosion than Wall #1. The total average surface compressive strength of Wall #1 and Wall #2 is 41.68 MPa and 37.39 MPa. These results support the hypothesis. However, the surface deterioration on Wall #1 was found to be 1.9% more than on Wall #2, which does not support the hypothesis. Considering the credibility of the method used to assess surface deterioration, more accurate tests are required to support the hypothesis.

### **Limitations of the Study and Future Scope**

The methodology used to assess the condition of SRE is limited by a number of factors. The material composition of the RE is unknown. If future investigation is to be completed on the FPH, the



moisture, soil, cement/lime content and insulation type should be determined. A U-value should be developed specific to these characteristics for a more accurate calculation of heat transfer.

Four data points were originally taken at Points 1 and 2 on Wall #1. The compressive strength difference was significant between surfaces at Point 1. This was an odd result, as Point 1 is the most shielded by its surroundings. This raised a question about the rebound hammer test and if the test was performed correctly. It is possible that rebound hammer did not impact the wall perpendicularly. The measurements at Points 1 and 2 were re-taken, and the sample size was increased for improved accuracy. Re-testing showed no change in results. Calibration of the rebound hammer could be performed on a known concrete sample however, the equipment had never been used prior to this study and so, it was assumed that the manufacturer provided adequate calibration.

The effectiveness of the high resolution photography method is dependent on the ability to highlight surface features, and differentiate between the natural texture of SRE and true weathering. It is not uncommon for SRE to look deteriorated, as friction between formworks during construction leaves a similar look. These effects should not be accounted for when analyzing surface deterioration from weathering however, it is difficult to differentiate between the two. It should also be noted that erosion is better quantified with depth, not surface area. For future investigation into SRE, erosion depth can be measured by using the stereo-photogrammetric method discussed by Bui [1].

True compressive strength and thermal properties should be determined by destructive testing. Thermocouples can be installed in and near the wall surfaces to obtain accurate temperature data, as wind, shade and other environmental factors can skew temperature readings. Liang found that an ultrasound device is more effective than a rebound hammer at measuring strength [7]. Performing an ultrasonic test should be considered if the FPH is to be further investigated. Additionally, a rebar locator should be used to confirm the rust sites on Wall #2.

Lastly, because the constituents of the RE mixture were unknown, it was impossible to go into an in-depth analysis on the technology specific to the FPH. For example, RE is often equipped with a vapour barrier to prevent moisture release and absorption. The effectiveness of the vapour barrier in the FPH is questionable due to the amount of efflorescence. Moisture content is extremely difficult to maintain due to the natural capillary effect, as stated by Hall [11]. Hall experimentally showed that thermal resistance decreases (poorer insulation) with increasing moisture content. This can be explained by the fact that the thermal conductivity of liquid water is significantly higher than that of air. Moisture is therefore an extremely important control parameter for maintaining thermal comfort and efficiency. Some suggestions can be made to waterproof future RE builds. Krystol Internal Membrane is a crystalline waterproofing admixture used to protect concrete against moisture transmission [15]. It is commonly used for concrete, but could be adopted for future use in SRE.

## **Concluding Remarks**

Presented in this article are methods used to non-destructively test two stabilized rammed earth walls at the First Peoples House. After 7 years of service, the eroded surface area on the exterior of the most eastern wall (Wall #1) is approximately 3.4%, and 1.8% on the most western wall (Wall #2). It is not uncommon for RE to appear deteriorated, as the surface is subjected to friction between formworks during construction. It should be noted that the effects of surface weathering are indistinguishable from the natural texture of RE. The thermal building envelope was analyzed using infrared imaging. The temperature difference between exterior and interior surfaces creates a driving potential for heat transfer and therefore a heat loss. If heat transfer rate is related to density, then the density at Point 2 on Wall #1, and Point 3 on Wall #2 is greatest. Heat loss rates at these locations were respectively

4.8 W/m<sup>2</sup>K and 4.0 W/m<sup>2</sup>K. The surface compressive strength of RE was measured using a rebound hammer. Large differences in strength existed between surfaces at Point 1 on Wall #1 and Point 3 on Wall #2. These results were not as expected. Measurements were re-taken but revealed no change in results. Relationships between wind loading and strength/surface deterioration were explored. Wind data was gathered to assess which walls have felt the most hours of between 2008-2015. This analysis revealed that Wall #2 experiences the most hours and the greatest wind speeds coming from 240-270° corresponding to the west-south-west and south-west poles. If wind direction and magnitude are proportional to wind loading, then Wall #2 should exhibit the greatest deterioration in strength and surface area. The results from the compressive strength and high resolution photography confirmed the hypothesis for strength deterioration, but did not favour surface deterioration. A number of alternative (and more accurate) testing methods were presented in this article, and should be considered for future analysis of the FPH. It was stated earlier that little literature is available on the condition of RE built within the last 10 years. This article acts as the first piece of literature to address the aging of 7 year old stabilized rammed earth construction in a BC climate.

## Acknowledgments

The authors wish to acknowledge Art Makosinski for providing the equipment needed to perform these tests; Tony Johnson, a professional in rammed earth who volunteered his time to support the study; and the staff at the First Peoples House for their cooperation.

## References

- [1] Bui, Q. B., Morel, J. C., Venkatarama, B. V., & Ghayad, W. (2009, May). Durability of rammed earth walls exposed for 20 years to natural weathering. *Building and Environment*, 44(5), 912-919.
- [2] SireWall Inc. (n.d.). *Insulated rammed earth - what is sirewall?* Retrieved 3 16, 2105, from SireWall: <http://www.sirewall.com/about/sirewall-system/>
- [3] Cianco, D. (2011). *Use of rammed earth in aboriginal remote communities of western Australia: a case study on sustainability and thermal properties*. University of Western Australia, School of Civil and Resource Engineering, Crawley.
- [4] Benhelal, E., Zahedi, G., Shamsaei, E., & Bahadori, A. (2013, July). Global strategies and potentials to curb CO<sub>2</sub> emissions in cement industry. *Journal of Cleaner Production*, 51, 142-161.
- [5] The Edmonton Journal. (2007, November 18). *Ancient rammed earth technology solidly green*. Retrieved from Canada.com: <http://www.canada.com/story.html?id=35970de2-b5fb-41a6-b755-9b5cf9dea936>
- [6] University of Victoria. (2008, August). *First Peoples House Brochure*. Retrieved from First Peoples House: <http://web.uvic.ca/fphouse/pdf/first-peoples-house-brochure-Aug08.pdf>
- [7] Liang, R., Hota, G., Lei, Y., Li, Y., Stanislawski, D., & Jiang, Y. (2013, January). Nondestructive Evaluation of Historic Hakka Rammed Earth Structures. *Sustainability*, 5, 298-315.

- [8] Proceq . (2015). *Operating Instructions Original Schmidt*. Retrieved 4 2015, 6, from Proceq: <http://www.proceq.com/en/site/downloads/Original%20Schmidt.html>
- [9] Mikron Instrument Company Inc. (2012). *Table of emissivity of various surfaces*. Retrieved from [http://www-eng.lbl.gov/~dw/projects/DW4229\\_LHC\\_detector\\_analysis/calculations/emissivity2.pdf](http://www-eng.lbl.gov/~dw/projects/DW4229_LHC_detector_analysis/calculations/emissivity2.pdf)
- [10] Bergman, T., Lavine, A., Incropera, F., & Dewitt, D. (2011). *Fundamentals of Heat and Mass Transfer* (Vol. 7). John Wiley & Sons Inc.
- [11] Hall, H., & Allinson, D. (2009, March). Assessing the effects of soil grading on the moisture content-dependent thermal conductivity of stabilised rammed earth materials. *Applied Thermal Engineering*, 29(4), 740-747.
- [12] Hall, M., & Djerbib, Y. (2006, July). Moisture ingress in rammed earth: Part 2 – The effect of soil particle-size distribution on the absorption of static pressure-driven water. *Construction and Building Materials*, 20(6), 374-383.
- [13] Government Of Canada. (n.d.). *Monthly Data Report, University of Victoria* . Retrieved from Canadian Climate Data : <http://climate.weather.gc.ca/>
- [14] Cimbala, J. M. (n.d.). *Conservation of Momentum using Control Volumes*. Retrieved from Fluid Mechanics Electronic Learning Supplement: [http://www.mne.psu.edu/cimbala/learning/fluid/cv\\_momentum/home.htm](http://www.mne.psu.edu/cimbala/learning/fluid/cv_momentum/home.htm)
- [15] Kryton International Inc. (2015). *Krystol Internal Membrane*. Retrieved 4 19, 2015, from Kryton: <http://www.kryton.com/products/krystol-internal-membrane-kim/>